
Optical spectroscopy of $\text{Li}_2\text{B}_4\text{O}_7$, CaB_4O_7 and LiCaBO_3 borate glasses doped with europium

^{1,2}Padlyak B.V., ²Kindrat I.I., ²Protsiuk V.O. and ²Drzewiecki A.

¹ Sector of Spectroscopy, Institute of Physical Optics, 23 Dragomanov Street, 79005 Lviv, Ukraine, bohdan@mail.lviv.ua

² Division of Spectroscopy of Functional Materials, Institute of Physics, University of Zielona Góra, 4a Szafrana Street, 65-516 Zielona Góra, Poland

Received: 02.05.2014

Abstract. We have investigated the optical properties (optical absorption, photoluminescence emission and excitation spectra, and luminescence kinetics) of a series of Eu-doped glasses with the compositions $\text{Li}_2\text{B}_4\text{O}_7$, CaB_4O_7 and LiCaBO_3 . $\text{Li}_2\text{B}_4\text{O}_7$:Eu, CaB_4O_7 :Eu and LiCaBO_3 :Eu glasses of high chemical purity and optical quality have been obtained from the corresponding polycrystalline compounds in the air atmosphere, using a standard glass technology. The Eu impurity has been introduced into the borate compounds in the form of Eu_2O_3 oxide in the amounts of 0.5 and 1.0 mol. %. On the basis of electron paramagnetic resonance and optical spectroscopy data we have shown that the impurity is incorporated into the glass network exclusively as Eu^{3+} ($4f^6$, 7F_0) ions. We have identified all $4f-4f$ transitions of the Eu^{3+} centres observed in the optical absorption and luminescence spectra. The most intense emission band of Eu^{3+} peaked about at 611 nm (the $^5D_0 \rightarrow ^7F_2$ transition) is characterized by a single exponential decay, with typical lifetimes that depend on the basic glass composition and the local structure of the luminescence centres Eu^{3+} . The peculiarities of the electron and local structures of the Eu centres in the $\text{Li}_2\text{B}_4\text{O}_7$, CaB_4O_7 and LiCaBO_3 glasses have been discussed and compared with the reference data for Eu-doped borate single crystals and polycrystalline compounds with the similar chemical compositions, as well as with other borate glasses.

Keywords: borate glasses, Eu^{3+} centres, optical absorption, luminescence, decay kinetics, local structure of luminescence centres

PACS: 78.55.Qr, 78.55.Qr, 78.20.Ci

UDC: 535.34+535.37+666.22

1. Introduction

Borate crystals and glasses, both undoped and doped with rare-earth and transition elements, are very promising materials for nonlinear optics and quantum electronics [1–6], scintillators, thermoluminescent dosimeters [7–11], gamma and neutron detectors [12–14], and many other applications. This especially applies to single crystals of lithium tetraborate ($\text{Li}_2\text{B}_4\text{O}_7$) characterized by extremely high radiation stability [15, 16], good thermoluminescent properties [9–11] and high transparency in the wide interval beginning from vacuum ultraviolet (UV) to middle infrared (IR) ranges [17].

The rare-earth ions such as Ce^{3+} , Eu^{3+} , Eu^{2+} , Er^{3+} , Nd^{3+} , Tm^{3+} , Sm^{3+} , Yb^{3+} , etc. reveal high luminescence efficiencies in various host materials and the emission in a broad enough spectral range. They are widely used as activator centres in different laser, luminescent and scintillate materials [18, 19], including Eu-doped borate crystals and glasses such as $\text{Li}_2\text{B}_4\text{O}_7$ [13, 14, 20–23], SrB_4O_7 [24, 25] and some others [26, 27]. One can also notice that crystalline and glassy (or

vitreous) oxide compounds are efficient luminescent materials for the ‘orange-red’ and ‘violet-blue’ spectral regions, when being activated with Eu^{3+} and Eu^{2+} ions, respectively.

On the other hand, the electron and local structures of impurity-associated paramagnetic and luminescence centres in crystals, glasses and other disordered compounds represent an interesting problem of the solid state physics and the spectroscopy of functional materials. The electron paramagnetic resonance (EPR) and the optical spectroscopy allow for investigating the electron and local structures of the paramagnetic and luminescence centres in single crystals and disordered solids, including glasses. To interpret the EPR and the optical spectra, and derive the electron and local structures of the luminescence and paramagnetic centres from the experimental spectra of glasses, one needs the structural and spectroscopic data of their crystalline analogues. The borate compounds represent suitable host materials for investigating the nature and the structure of the luminescence and paramagnetic centres, because virtually all of the borates ($\text{Li}_2\text{B}_4\text{O}_7$, $\text{K}_2\text{B}_4\text{O}_7$, KLiB_4O_7 , LiCaBO_3 , CaB_4O_7 , SrB_4O_7 etc.) can be obtained in both crystalline and glassy (or vitreous) phases. Furthermore, the glassy borate compounds are more promising when compared with their crystalline analogues from the technological point of view, since the growth of borate single crystals is a difficult, long-term and so very expensive process. Besides, a very low velocity of the crystal growth and a high viscosity of the melt impose the problems of doping the borate crystals with the rare-earth and transition elements. On the other hand, these problems are completely absent for the case of glassy borate compounds.

Up to now the optical and luminescent properties of crystalline and glassy Eu-doped borate compounds with different chemical compositions have been extensively investigated in a number of works [20–37]. Let us remind of the main results. Ref. [14] has reported a synthesis, optical and luminescence properties, and some scintillation characteristics associated with detecting neutrons ($E_n \leq 10$ MeV) and ^{60}Co γ -radiation for the case of undoped and Eu-, Cu-, Ce-, Sm-, Tb-, Tm- and Yb-doped lithium tetraborate ($\text{Li}_2\text{B}_4\text{O}_7$) glasses. Preparation and spectroscopic properties of Eu^{3+} -doped lithium borate glasses have been reported in Refs. [20, 21]. The changes occurring in the optical properties and the valence state of Eu impurity in the $\text{Li}_2\text{B}_4\text{O}_7$:Eu glasses have been described in Ref. [21] depending on the glass synthesis atmosphere. Different fluorescence properties of Eu-doped crystal and glass with the composition La_2O_3 – $3\text{B}_2\text{O}_3$ have been explained by different local structures around the Eu^{3+} ions [23]. In particular, the Eu^{3+} ions form a complex Eu^{3+} – O^{2-} – B^{3+} bond in the glass network, whereas Eu^{3+} ions in the crystal lattice form a complex Eu^{3+} – O^{2-} – La^{3+} bond. According to the data [23], the luminescence lifetime values for the Eu^{3+} ions in the crystal and the glass are different, being equal respectively to 3.08 and 1.98 ms. The optical and EPR studies for the Eu- and Pr-doped glasses with the compositions SrO – $2\text{B}_2\text{O}_3$ or SrB_4O_7 have been reported in Ref. [24]. Basing on the optical absorption and luminescence spectra, it has been shown that the Eu impurity is incorporated into the SrB_4O_7 glass network exclusively in the trivalent state, Eu^{3+} ($4f^6$, $^7\text{F}_0$) [24]. According to the results [24], the luminescence kinetics for the SrB_4O_7 :Eu glass manifests only isolated (or single) Eu^{3+} centres, whereas a double exponential decay caused by the single (Eu^{3+}) and the pair (Eu^{3+} – Eu^{3+}) centres is characteristic for the polycrystalline SrB_4O_7 :Eu compound. The luminescence excitation and the emission spectra of polycrystalline LiCaBO_3 : M^{3+} ($\text{M}^{3+} = \text{Eu}^{3+}$, Sm^{3+} , Tb^{3+} , Ce^{3+} and Dy^{3+}) compounds, which represent phosphors promising for the white-light LED, have been investigated in Ref. [26].

The main features of the synthesis and the luminescence properties of SrB_4O_7 :Eu, Tb phosphors have been reported in the work [25]. If compared with the Eu^{3+} emission, the relative intensity of the Eu^{2+} emission increases when Tb^{3+} ions are incorporated in the SrB_4O_7 :Eu compound

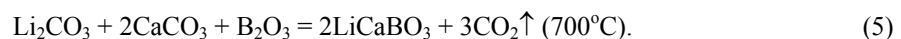
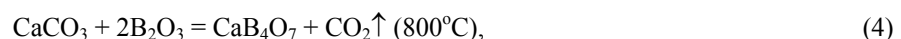
[25]. The undoped and Eu-doped zinc borate glasses of different compositions prepared using a melt-quenching technique in the air atmosphere have been studied in Ref. [27]. In the Eu-doped zinc borate glasses, increasing Eu impurity concentration leads to gradual disappearance of the broad-band emission in the near-UV spectral region, while the ‘red’ Eu^{3+} emission increases considerably [27]. According to the data [28], Sm^{3+} and Eu^{3+} ions are reduced to the divalent state by negatively charged vacancies produced in the borate and phosphate matrices, with the structures containing tetragonal AO_4 ($A = \text{B}$ and P) groups. Reduction of the Eu^{3+} ions to Eu^{2+} in the process of growth of the SrB_4O_7 single crystals based on the top-seeded solution method has been reported by the authors [29]. The effect of irradiation dose on the $\text{Eu}^{3+} \rightarrow \text{Eu}^{2+}$ reduction in the aluminoborosilicate glasses has been investigated in Ref. [30]. The EPR measurements have confirmed a strong increase in the quantity of Eu^{2+} ions with increasing irradiation dose [30]. The study [31] has demonstrated that the host-matrix modification determines crucially the valence state of europium and the luminescence characteristics of the relevant materials. The photoluminescence spectrum of the $\text{Li}_2\text{B}_4\text{O}_7:\text{Eu}$ single crystals shows a single broad-band ‘violet-blue’ emission corresponding to the Eu^{2+} centres. It is peaked at 370 nm and has the lifetime of 24 μs . A characteristic series of ‘red’ emission lines related to the Eu^{3+} centres has been observed for the $\text{Li}_2\text{B}_4\text{O}_7:\text{Eu}$ glasses, with the lifetime of 2.2 ms [31].

Using the data available in the literature, we have concluded that the spectroscopic properties of the Eu-doped borate glasses are not studied in a sufficient detail. In particular, the features of the electron and local structures of the luminescent Eu centres in the network of borate glasses with different compositions seem to be not satisfactorily investigated. Therefore, the main aim of this work is to study the spectroscopic properties of Eu-doped borate glasses with different compositions and Eu concentrations, and to determine the electron and local structures of Eu centres in those glasses using the EPR and the optical spectroscopy methods.

2. Experimental details

2.1. Glass synthesis and preparation of samples

Eu-doped borate glasses $\text{Li}_2\text{O}-\text{B}_2\text{O}_3$ (or $\text{Li}_2\text{B}_4\text{O}_7$), $\text{CaO}-2\text{B}_2\text{O}_3$ (or CaB_4O_7) and $\frac{1}{2}(\text{Li}_2\text{O}-2\text{CaO}-\text{B}_2\text{O}_3)$ (or LiCaBO_3) were obtained in the air atmosphere from the corresponding polycrystalline compounds. Standard glass synthesis technique, corundum crucibles and technological conditions were used, as described in Ref. [32]. For the solid-state synthesis of polycrystalline compounds $\text{Li}_2\text{B}_4\text{O}_7:\text{Eu}$, $\text{CaB}_4\text{O}_7:\text{Eu}$ and $\text{LiCaBO}_3:\text{Eu}$ we employed Li_2CO_3 and CaCO_3 carbonates, and a boric acid (H_3BO_3) of a high chemical purity (99.999%, Aldrich). Eu impurity was added to the raw materials in the form of Eu_2O_3 oxide of a chemical purity (99.99%). The relevant amounts were 0.5 and 1.0 mol. %. The solid-state synthesis of the polycrystalline borate compounds was carried out using multi-step heating reactions [32]. For the cases of $\text{Li}_2\text{B}_4\text{O}_7$, CaB_4O_7 and LiCaBO_3 these may be described by the following chemical equations:



Large samples of $\text{Li}_2\text{B}_4\text{O}_7:\text{Eu}$, $\text{CaB}_4\text{O}_7:\text{Eu}$ and LiCaBO_3 glasses were obtained after cooling rapidly the corresponding melts heated to more than 100 K above the melting points ($T_{\text{melt}} = 917^\circ\text{C}$

(1190 K), 980°C (1253 K) and 777°C (1050 K) for $\text{Li}_2\text{B}_4\text{O}_7$, CaB_4O_7 and LiCaBO_3 compounds, respectively) to make crystallisation processes impossible [32]. Two types of crucibles, graphite (C) and corundum ceramic (Al_2O_3) ones, were used for obtaining the borate glasses. The optical quality of the glasses thus obtained was practically independent of the type of crucibles. The glass samples for the spectroscopic investigations were cut to the approximate sizes of $5 \times 4 \times 2 \text{ mm}^3$ and then polished.

2.2. Experimental equipment and characterization of samples

The paramagnetic impurities in our glasses $\text{Li}_2\text{B}_4\text{O}_7:\text{Eu}$, $\text{CaB}_4\text{O}_7:\text{Eu}$ and $\text{LiCaBO}_3:\text{Eu}$ were detected with the EPR technique, using modernized commercial X-band radiospectrometers SE/X-2013 and SE/X-2544 (RADIOPAN, Poznań, Poland). They operated in a high-frequency (100 kHz) modulation mode for the magnetic field at the room temperature (RT). The working microwave frequency of the radiospectrometers was measured using a Hewlett Packard (model 5350 B) frequency counter and a DPPH g -marker ($g = 2.0036 \pm 0.0001$).

The optical absorption spectra of the $\text{Li}_2\text{B}_4\text{O}_7:\text{Eu}$, $\text{CaB}_4\text{O}_7:\text{Eu}$ and $\text{LiCaBO}_3:\text{Eu}$ glasses were recorded with a Varian (model 5E UV-VIS-NIR) and SHIMADZU (model 2450 UV-VIS) spectrophotometers. The luminescence (both the excitation and emission) spectra and the luminescence kinetics of our glasses were detected in the UV and visible spectral ranges at the RT, using a HORIBA spectrofluorimeter (model FluoroMax-4).

It is known that the undoped tetraborate glass $\text{Li}_2\text{B}_4\text{O}_7$ is characterized by high transparency in the spectral region 281–2760 nm [14]. According to Ref. [33], the undoped $\text{Li}_2\text{B}_4\text{O}_7$ glass is transparent at 300–2500 nm, whereas the nominally pure $\text{Li}_2\text{B}_4\text{O}_7$ single crystal at 167–3200 nm. The $\text{Li}_2\text{B}_4\text{O}_7:\text{Eu}$, $\text{CaB}_4\text{O}_7:\text{Eu}$ and $\text{LiCaBO}_3:\text{Eu}$ glasses are almost not coloured and are characterized by a high optical quality. The nominal Eu-dopant concentrations have not been proved analytically, though our previous studies [34, 35] have shown that the coefficient of incorporation of the rare-earth impurities into the borate glass network is close to unity. The characteristic optical spectra (the absorption, luminescence excitation and the emission) and the luminescence kinetics for the $\text{Li}_2\text{B}_4\text{O}_7:\text{Eu}$, $\text{CaB}_4\text{O}_7:\text{Eu}$ and $\text{LiCaBO}_3:\text{Eu}$ glasses will be discussed in Section 3.1.

Notice that EPR signals with $g_{\text{eff}} \cong 4.3$ and $g_{\text{eff}} \cong 2.0$ are detected for all of our $\text{Li}_2\text{B}_4\text{O}_7:\text{Eu}$, $\text{CaB}_4\text{O}_7:\text{Eu}$ and $\text{LiCaBO}_3:\text{Eu}$ glasses. The integral intensity of the EPR signal with $g_{\text{eff}} \cong 4.3$ observed in the Eu-doped glasses is notably (approximately 10–20 times) larger than that of the signal with $g_{\text{eff}} \cong 2.0$. According to Refs. [36, 37], the EPR signal with $g_{\text{eff}} \cong 4.3$ is characteristic for the glassy compounds and refers to the isolated uncontrolled impurity ions Fe^{3+} ($3d^5$, ${}^6\text{S}_{5/2}$) localized at the octahedral and/or tetrahedral sites of the glass network with a strong rhombic distortion. The presence of the Fe^{3+} EPR signal with $g_{\text{eff}} \cong 4.3$ clearly demonstrates a typical glass structure of the $\text{Li}_2\text{B}_4\text{O}_7:\text{Eu}$, $\text{CaB}_4\text{O}_7:\text{Eu}$ and $\text{LiCaBO}_3:\text{Eu}$ compounds. A broader EPR signal with $g_{\text{eff}} \cong 2.0$ is related to the pair $\text{Fe}^{3+}-\text{Fe}^{3+}$ centres coupled through a magnetic dipolar interaction [36]. The uncontrolled Fe^{3+} impurity ions are characterized by very weak spin-forbidden absorption transitions in the UV and ‘blue’ spectral regions. Therefore they do not manifest themselves in the optical absorption and the luminescence excitation spectra of the glasses under test.

3. Results and discussion

3.1. Optical spectra and luminescence kinetics of the Eu-doped borate glasses

The preliminary results of our spectroscopic studies for the Eu-doped lithium tetraborate glasses were reported in brief in Ref. [34]. The EPR and the optical spectra of the $\text{CaB}_4\text{O}_7:\text{Eu}$ and

LiCaBO₃:Eu glasses have not yet been investigated. In general, the europium impurity can incorporate into the structures of different oxide compounds as paramagnetic Eu²⁺ (4f⁷, ⁸S_{7/2}) or non-paramagnetic Eu³⁺ (4f⁶, ⁷F₀). The electron structure of the paramagnetic Eu²⁺ ions is the same as that of Gd³⁺ and Tb⁴⁺ (4f⁷, ⁸S_{7/2}) ions. All of these ions can be easily detected in the glasses and crystals with the aid of the EPR technique, even at the RT. Characteristic signal of the paramagnetic Eu²⁺ centres has been not observed in the EPR spectra of the Li₂B₄O₇:Eu, CaB₄O₇:Eu and LiCaBO₃:Eu glasses. Hence, we conclude that the Eu impurity is incorporated in the network of our borate glasses exclusively as Eu³⁺ ions.

The spectroscopic properties of the centres Eu³⁺ are clearly revealed in the characteristic optical spectra of Li₂B₄O₇:Eu, CaB₄O₇:Eu and LiCaBO₃:Eu glasses. Notice that the optical absorption, emission and luminescence excitation spectra, together with the luminescence kinetics presented below, also confirm that the Eu impurity is incorporated in the structure of our borate glasses in its trivalent (Eu³⁺) state.

In the 350÷2250 nm region and at the RT, the optical absorption spectra of our Eu-doped glasses consist of an intense broad absorption band and several weak absorption bands. The optical absorption spectrum typical of the Li₂B₄O₇:Eu glass containing 1.0 mol. % Eu₂O₃ is presented in Fig. 1. The intense broad absorption band is assigned to the charge transfer O²⁻ → Eu³⁺ and, simultaneously, to the fundamental absorption of the host glass. The charge-transfer band corresponds to the electron transfer from the oxygen (O²⁻) 2p orbital to the empty orbital of the Eu³⁺ ions. In general, the position of the charge-transfer band is defined by the local structure of the rare-earth ion. It is known that the position of the charge-transfer band depends on the Eu³⁺ coordination number and the interatomic distance Eu–O [38]. The local structure of the Eu³⁺ centres in our borate glasses will be discussed in Section 3.2.

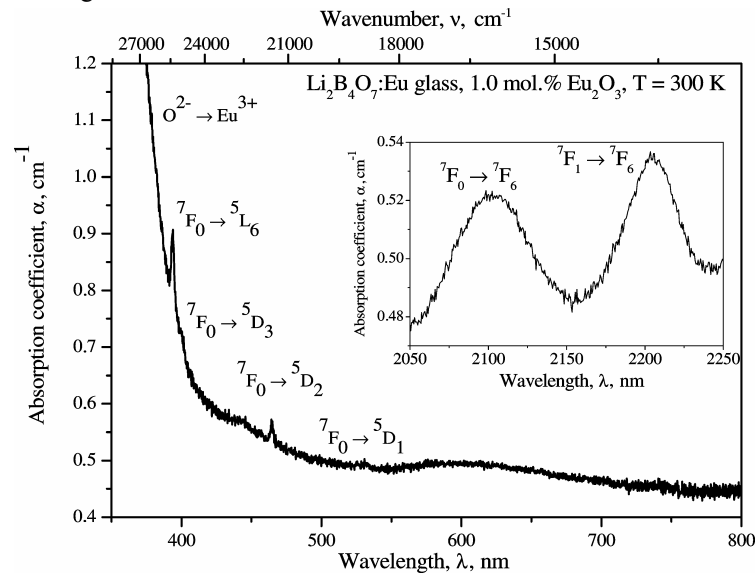


Fig. 1. Optical absorption spectrum for the Li₂B₄O₇:Eu glass containing 1.0 mol. % Eu₂O₃, measured at T=300K.

In accordance with the data [39, 40], weakly resolved absorption bands observed for our glasses should be assigned to the absorption transitions ⁷F₀ → ⁵L₆, ⁷F₀ → ⁵D₃, ⁷F₀ → ⁵D₂, ⁷F₀ → ⁵D₁, ⁷F₀ → ⁷F₆ and ⁷F₁ → ⁷F₆ (see Fig. 1). Some of the absorption bands are only weakly revealed in the optical absorption spectra (see Fig. 1), but all of these bands are clearly observed in the luminescence excitation spectra presented in Fig. 2.

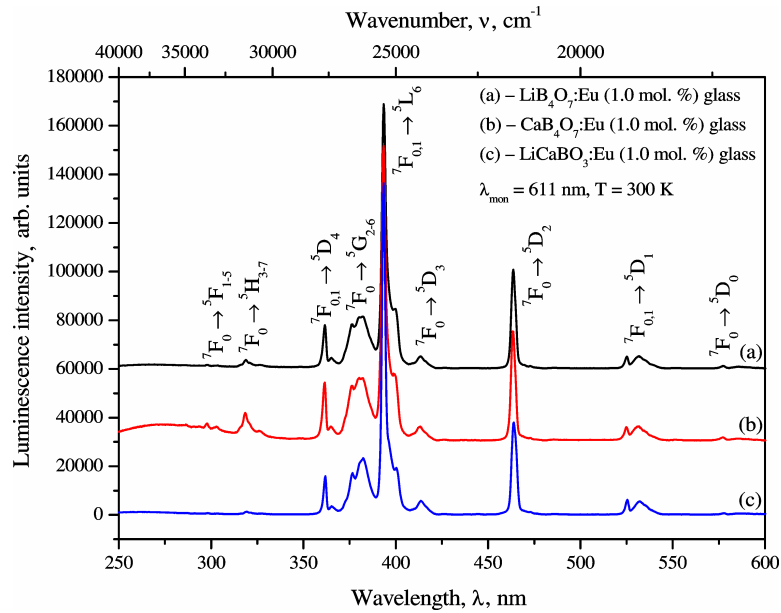


Fig. 2. Luminescence excitation spectra of Eu^{3+} centres in the $\text{Li}_2\text{B}_4\text{O}_7:\text{Eu}$ (a), $\text{CaB}_4\text{O}_7:\text{Eu}$ (b) and $\text{LiCaBO}_3:\text{Eu}$ (c) glasses containing 1.0 mol. % Eu_2O_3 , measured at $\lambda_{\text{mon}} = 611 \text{ nm}$ (${}^5\text{D}_0 \rightarrow {}^7\text{F}_2$ transition) and $T = 300 \text{ K}$.

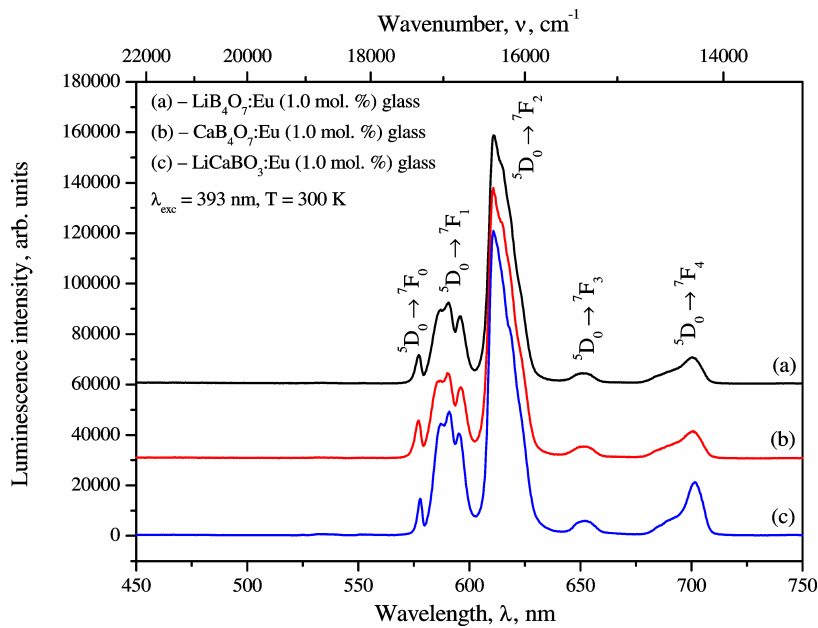


Fig. 3. Emission spectra of Eu^{3+} centres in the $\text{Li}_2\text{B}_4\text{O}_7:\text{Eu}$ (a), $\text{CaB}_4\text{O}_7:\text{Eu}$ (b) and $\text{LiCaBO}_3:\text{Eu}$ (c) glasses containing 1.0 mol. % Eu_2O_3 . Spectra are measured under excitation with $\lambda_{\text{exc}} = 393 \text{ nm}$ (${}^7\text{F}_0 \rightarrow {}^5\text{L}_6$ transition) at $T = 300 \text{ K}$.

The emission spectra of $\text{Li}_2\text{B}_4\text{O}_7$, CaB_4O_7 and LiCaBO_3 glasses containing 0.5 and 1.0 mol.% Eu_2O_3 are quite similar. The influence of the impurity concentration on the luminescent properties of Eu^{3+} ions is negligible and leads only to slightly different intensities of the emission bands. That is why Fig. 3 presents the emission spectra of the glasses containing only 1.0 mol. % Eu_2O_3 . They demonstrate the influence of the glass network on the intensity of luminescence bands of the Eu^{3+} centres.

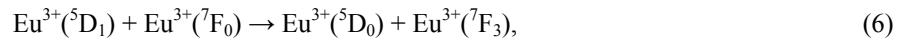
The emission spectra measured under the same experimental conditions ($T = 300$ K and $\lambda_{\text{exc}} = 393$ nm) exhibit five characteristic emission bands of the Eu^{3+} ions in the region of 570–710 nm (see Fig. 3). In accordance with the energy level diagram for Eu^{3+} and the data [39, 40], the emission bands correspond to the ${}^5\text{D}_0 \rightarrow {}^7\text{F}_J$ ($J = 0\div 4$) f - f transitions of Eu^{3+} ions, which are indicated in Fig. 3.

When a rare-earth ion occupies a site with the inversion symmetry, the selection rules have the well-known form: $\Delta J = 0, \pm 1$ [18]. In the cases when $\Delta J = 0$, any transitions to the state with $J = 0$ are forbidden, too. All of these transitions are magnetic dipole ones. In the lattice with no inversion symmetry there can appear electric dipole transitions. The selection rules for these transitions are as follows: $\Delta J = 0, \pm 2, \pm 4$, or ± 6 [41]. Furthermore, the electric dipole transitions are forbidden for the ground and excited states characterized with $J = 0$.

In other words, the relative intensities of the luminescence bands due to the electric and magnetic dipole transitions of Eu^{3+} change depending on the crystal symmetry of the host materials [41]. The ${}^5\text{D}_0 \rightarrow {}^7\text{F}_J$ transitions of Eu^{3+} ions are ideally suitable when determining the symmetry of the lattice sites [42]. Namely, the electric dipole transitions among the $4f$ levels are strictly forbidden for the positions having the inversion symmetry. If the inversion symmetry is broken, there appear the electric dipole transitions. They will dominate in the spectrum even if the symmetry deviates only slightly from the inversion one [42].

In the emission spectra studied in this work (see Fig. 3), the main emission band peaked nearby 611 nm is assigned to the ${}^5\text{D}_0 \rightarrow {}^7\text{F}_2$ electric dipole transition in Eu^{3+} , while the emission near 592 nm corresponds to the magnetic dipole transition ${}^5\text{D}_0 \rightarrow {}^7\text{F}_1$. Notice that the relative intensity of the ${}^5\text{D}_0 \rightarrow {}^7\text{F}_1$ transition in the $\text{LiCaBO}_3:\text{Eu}$ glass is higher than that for the $\text{Li}_2\text{B}_4\text{O}_7:\text{Eu}$ and $\text{CaB}_4\text{O}_7:\text{Eu}$ glasses (see Fig. 3). The emission intensities of the ‘red’ and ‘orange’ bands corresponding to the ${}^5\text{D}_0 \rightarrow {}^7\text{F}_2$ and ${}^5\text{D}_0 \rightarrow {}^7\text{F}_1$ transitions is known to be ‘asymmetric’. High ‘asymmetry’ is favourable while improving colour purity of the red phosphors [18]. Considering a dominance of the ‘red’ emission, extremely high radiation stability [15, 16] and high transparency of Eu-doped borate glasses in the wide spectral range, one can argue that these glasses represent a promising ‘red’ luminescent material.

The dominance of the ‘red’ emission associated with the ${}^5\text{D}_0 \rightarrow {}^7\text{F}_2$ transition indicates the inversion antisymmetric crystal field. In its turn, this implies very low site symmetry of the Eu^{3+} centres in our borate glasses. The presence of the forbidden ${}^5\text{D}_0 \rightarrow {}^7\text{F}_0$ and ${}^5\text{D}_0 \rightarrow {}^7\text{F}_3$ transitions in the emission spectra can be explained by ‘mixing’ of the $J = 0$ and $J = 3$ states with the other states, which can be induced by the crystal field. The absence of the emission from the higher ${}^5\text{D}_J$ ($J \geq 1$) levels may be related to multi-phonon relaxation from the higher excited levels to the state ${}^5\text{D}_0$, or cross-relaxation processes described by the relation [18]



which are caused by relatively high concentrations of Eu^{3+} in the glass network.

The luminescence excitation spectra of the Eu^{3+} centres in $\text{Li}_2\text{B}_4\text{O}_7$, CaB_4O_7 and LiCaBO_3 containing 1.0 mol. % Eu_2O_3 detected with the same experimental setup as above ($T = 300$ K and $\lambda_{\text{mon}} = 611$ nm) are shown in Fig. 2. The influence of impurity concentration on the luminescent properties of Eu^{3+} centres is insignificant and imposes only slightly different intensities of the excitation bands. Therefore the luminescence excitation spectra for the borate glasses containing 0.5 mol. % Eu_2O_3 are not presented in Fig. 2.

According to the energy level diagram and the data [39, 40], the observed luminescence

excitation bands are assigned to the electronic $f-f$ transitions of Eu^{3+} . They are indicated in Fig. 2. The main excitation bands are assigned to the transitions ${}^7\text{F}_{0,1} \rightarrow {}^5\text{L}_6$ and ${}^7\text{F}_0 \rightarrow {}^5\text{D}_J$ ($J = 0-4$) of Eu^{3+} ions. The Eu^{3+} luminescence excitation bands reveal sufficient correlation with the corresponding optical absorption bands (cf. Fig. 1 and Fig. 2).

Rather weak resolution of some bands in the Eu^{3+} luminescence excitation spectra is related to inhomogeneous broadening caused by structural disordering of the glass host, which leads to slightly different local surroundings and crystal field parameters for different Eu^{3+} centres available in the glass network. As a result, some weakly resolved Eu^{3+} bands are assigned to the groups of optical transitions (see Fig. 2). It should be noted that the excitation bands from a higher ${}^7\text{F}_1$ level are also present in the excitation spectra. They are caused by a smallness of energy distance between the ${}^7\text{F}_0$ and ${}^7\text{F}_1$ levels that increases the probability of thermal excitation at the RT.

The intensity of the charge-transfer band peaked near 260 nm is very weak for $\text{Li}_2\text{B}_4\text{O}_7:\text{Eu}$ and $\text{LiCaBO}_3:\text{Eu}$ and slightly higher for $\text{CaB}_4\text{O}_7:\text{Eu}$ (see Fig. 2). Comparing the relative intensities of the charge-transfer band and the $f-f$ bands of Eu^{3+} ions in the glasses under study, we note that the intensity of the $f-f$ bands is higher. This is opposite to that occurring in the lithium borate crystals where, according to Ref. [23], the intensity of the charge-transfer band is stronger than that of the $f-f$ bands.

Thus, the emission and luminescence excitation spectra also testify that the europium impurity is incorporated in the $\text{Li}_2\text{B}_4\text{O}_7$, CaB_4O_7 and LiCaBO_3 glass network exclusively as Eu^{3+} ions. This agrees well with the data known for the Eu-doped lithium tetraborate crystal [22], the lithium tetraborate glass [31], the lithium borate glasses [20, 23, 43] and the other borate glasses [24, 44, 45]. However, the above result does not correlate with the findings for the Eu-doped $\text{Li}_2\text{B}_4\text{O}_7$ [31] and SrB_4O_7 [29] crystals, the lithium borate glasses [21] and some other borate glasses [28, 30]. Those works have testified the additional presence of the luminescence centres Eu^{2+} .

The luminescence kinetics of Eu^{3+} in the $\text{Li}_2\text{B}_4\text{O}_7$, CaB_4O_7 and LiCaBO_3 glasses containing 0.5 and 1.0 mol. % Eu_2O_3 has been studied at $\lambda_{\text{exc}} = 393$ nm, $\lambda_{\text{mon}} = 611$ nm ($T = 300$ K). It is depicted in Fig. 4 on a semi-logarithmic scale. As seen from Fig. 4, the decay curves for the most intense ‘orange-red’ emission band (the ${}^5\text{D}_0 \rightarrow {}^7\text{F}_2$ transition) peculiar for all of the glasses can be described satisfactory by a single exponent. The relevant lifetimes are $\tau = (2.25 \pm 0.02)$ ms and $\tau = (2.26 \pm 0.02)$ ms for $\text{Li}_2\text{B}_4\text{O}_7:\text{Eu}$, $\tau = (2.11 \pm 0.02)$ ms and $\tau = (2.12 \pm 0.02)$ ms for $\text{CaB}_4\text{O}_7:\text{Eu}$, and $\tau = (2.04 \pm 0.02)$ ms and $\tau = (2.07 \pm 0.02)$ ms for $\text{LiCaBO}_3:\text{Eu}$. Here the first and the second figures refer to the samples containing 0.5 and 1.0 mol. % Eu_2O_3 , respectively.

The luminescence decay curves and the lifetime values correspond to the same type of Eu^{3+} centres, with slightly different parameters due to inhomogeneous broadening of the spectral lines. The same lifetime values obtained for the $\text{Li}_2\text{B}_4\text{O}_7:\text{Eu}$, $\text{CaB}_4\text{O}_7:\text{Eu}$ and $\text{LiCaBO}_3:\text{Eu}$ glasses with different Eu_2O_3 concentrations clearly demonstrate that the interaction $\text{Eu}^{3+}-\text{Eu}^{3+}$ is absent or negligible even in the samples with a relatively high (1.0 mol. %) concentration of Eu_2O_3 . This result shows homogeneous distribution of the Eu^{3+} centres without pairing and clustering in the $\text{Li}_2\text{B}_4\text{O}_7:\text{Eu}$, $\text{CaB}_4\text{O}_7:\text{Eu}$ and $\text{LiCaBO}_3:\text{Eu}$ borate glass network.

The luminescence decay curves provide important information linked with influence of the glass host and the europium content on the lifetime values for the lithium and calcium borate glasses. These points have yet not been reliably studied in the literature. Notice that the lifetimes obtained for the ${}^5\text{D}_0 \rightarrow {}^7\text{F}_2$ transition of Eu^{3+} centres in the $\text{Li}_2\text{B}_4\text{O}_7:\text{Eu}$, $\text{CaB}_4\text{O}_7:\text{Eu}$ and $\text{LiCaBO}_3:\text{Eu}$ glasses are consistent with the data [46]. According to Ref. [46], the lifetimes for the borate and fluoroborate glasses containing lithium, zinc and lead depend on the glass composition,

lying in the 1.17–2.36 ms region. For the Eu-doped borate glasses with different compositions, the following lifetimes have been reported: 2.2 ms for $\text{Li}_2\text{B}_4\text{O}_7:\text{Eu}$ glass [31], 2.093 ms for $\text{Li}_3\text{BO}_3:\text{Eu}$ glass [47], 3.08 and 1.89 ms respectively for $\text{La}_2\text{O}_3\text{--}3\text{B}_2\text{O}_3:\text{Eu}$ crystal and glass [23], 1.82 ms for $\text{SrB}_4\text{O}_7:\text{Eu}$ glass [24], and 2.35 ms for zinc-lead borate glass [48].

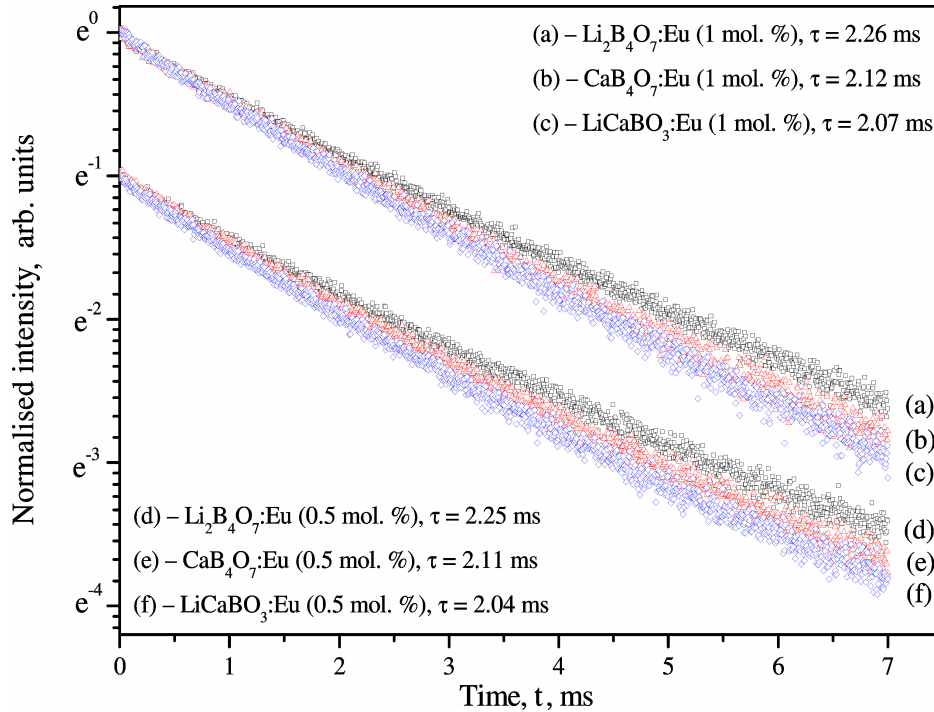


Fig. 4. Luminescence decay curves for Eu^{3+} centres (${}^5\text{D}_0 \rightarrow {}^7\text{F}_2$ transition, $\lambda_{\text{mon}} = 611 \text{ nm}$) in the $\text{Li}_2\text{B}_4\text{O}_7:\text{Eu}$, $\text{CaB}_4\text{O}_7:\text{Eu}$ and $\text{LiCaBO}_3:\text{Eu}$ glasses containing 1.0 (curves a, b, c) and 0.5 mol. % Eu_2O_3 (curves d, e, f), measured at $T = 300 \text{ K}$ under excitation with $\lambda_{\text{exc}} = 393 \text{ nm}$ (${}^7\text{F}_0 \rightarrow {}^5\text{L}_6$ transition).

The Eu^{3+} centres in our glasses show considerably shorter lifetimes. Ordering the glass compositions from the highest to the lowest lifetime values, we arrive at the sequence $\text{Li}_2\text{B}_4\text{O}_7:\text{Eu}$, $\text{CaB}_4\text{O}_7:\text{Eu}$ and $\text{LiCaBO}_3:\text{Eu}$ (see Fig. 4 a, b, c and d, e, f). Our results for the luminescence kinetics show distinctly that the glass host influences the lifetime of the Eu^{3+} centres which are localized at the same Li(Ca) sites of the glass network. The dependence of the lifetime on the local structure of Eu^{3+} centres in the $\text{Li}_2\text{B}_4\text{O}_7$, CaB_4O_7 and LiCaBO_3 glasses is considered in Section 3.2.

3.2. Local structure of luminescence Eu^{3+} centres in the borate glasses

Using direct EXAFS (Extended X-ray Absorption Fine Structure) studies of the L_3 edge of the rare-earth impurity ions, the authors of Ref. [49] have shown that the local structures (the first coordination shells) of the rare-earth ions are closely similar in the oxide crystals and glasses with the same chemical composition. In particular, this is valid for the crystal and glass $\text{Ca}_3\text{Ga}_2\text{Ge}_3\text{O}_{12}$ (or $3\text{CaO--Ga}_2\text{O}_3\text{--}3\text{GeO}_2$). As a consequence, the local structures of the impurity luminescence centres Eu^{3+} in the network of our borate glasses will be considered basing on the analysis of structural data for the $\text{Li}_2\text{B}_4\text{O}_7$, CaB_4O_7 and LiCaBO_3 glasses [32, 50] and their crystalline analogues [51–53].

The local structures of cationic sites in the $\text{Li}_2\text{B}_4\text{O}_7$, CaB_4O_7 and LiCaBO_3 glasses have been described in detail in Refs. [32, 50] and compared with the corresponding structures for their

crystalline analogues. According to Refs. [32, 50], boron atoms in the $\text{Li}_2\text{B}_4\text{O}_7$ glass are in general fourfold-coordinated (tetrahedral BO_4 units), with the average interatomic distance B–O equal to 0.165 nm. A certain proportion of threefold-coordinated B atoms (triangular BO_3 units) with shorter B–O distances are also present in the $\text{Li}_2\text{B}_4\text{O}_7$ glass network. The local environment of Li atoms in the $\text{Li}_2\text{B}_4\text{O}_7$ glass also consists of tetrahedral oxygen units with the average Li–O distance equal to 0.279 nm. This agrees with the appropriate distances in the first coordination shell found for Li atoms in the $\text{Li}_2\text{B}_4\text{O}_7$ single crystal [32].

The local structure of the cationic sites has not yet been studied for the CaB_4O_7 glass. For characterization of this compound, one can use the structural data [32, 50] for the isomorphous SrB_4O_7 glasses. According to the structural data available for those glasses [32, 50] and the crystals with the same composition [52], the structure of the CaB_4O_7 glasses may be supposed to consist of BO_4 tetrahedra, with the average B–O distance equal to about 0.140 nm. Two types of BO_4 tetrahedra with similar B–O distances, which are characteristic for the crystal lattice of SrB_4O_7 [52], have not been resolved in the intensity curve and the pair correlation function for the SrB_4O_7 glass [32]. The Sr–O distances in the SrB_4O_7 crystal are in the region of 0.273–0.339 nm [52]. The coordination number to oxygen for Sr atoms depends on the Sr–O distances and equals to four when the radius of the first coordination shell is less than 0.290 nm [52]. According to Refs. [32, 52], Sr(Ca) atoms should be stabilized in the SrB_4O_7 (CaB_4O_7) glass network at the sites with the coordination number $N = 4$ to oxygen, where the average distance Sr–O (Ca–O) is equal to about 0.262 nm [32].

In the LiCaBO_3 glass network the boron atoms form triangular BO_3 units with the average interatomic distance B–O of 0.149 nm [32, 50]. Ca atoms are located at the sites with the coordination number $N = 6\text{--}7$, with the average Ca–O distance being equal to 0.258 nm [32]. Li atoms are located at the sites with the coordination number $N = 4\text{--}5$ (the average Li–O distance should be less than 0.258 nm) [32]. The average distances B–O and Ca–O obtained for the LiCaBO_3 glass [32] correlate well with the corresponding parameters known for its crystalline analogue [53].

Basing on the structural data for the $\text{Li}_2\text{B}_4\text{O}_7$, CaB_4O_7 (SrB_4O_7) and LiCaBO_3 crystals [51–53], one can suppose that the trivalent rare-earth impurity ions RE^{3+} in these borate crystals can be incorporated only at the Li^+ (Ca^{2+} , Sr^{2+}) lattice sites, due to extremely small ionic radius of B^{3+} ions (0.23 Å). Then the Eu^{3+} ions are expected to incorporate into the Li^+ (Ca^{2+}) sites of the $\text{Li}_2\text{B}_4\text{O}_7$, CaB_4O_7 and LiCaBO_3 lattices, since the ionic radii of Li^+ (Ca^{2+}) and Eu^{3+} are close to each other and approximately equal to 0.76 (1.00) Å and 0.95 Å, respectively. According to the structural data known for the borate glasses [32, 50] and their crystalline analogues [51–53], as well as the results of EXAFS studies of the local structure of RE^{3+} impurity ions in the oxide glass and crystal with the composition $\text{Ca}_3\text{Ga}_2\text{Ge}_3\text{O}_{12}$ [49], one can state that the Eu^{3+} ions are incorporated into the Li^+ (Ca^{2+}) sites of $\text{Li}_2\text{B}_4\text{O}_7$, CaB_4O_7 and LiCaBO_3 glasses (see Fig. 5). Compensation of the excess positive charges

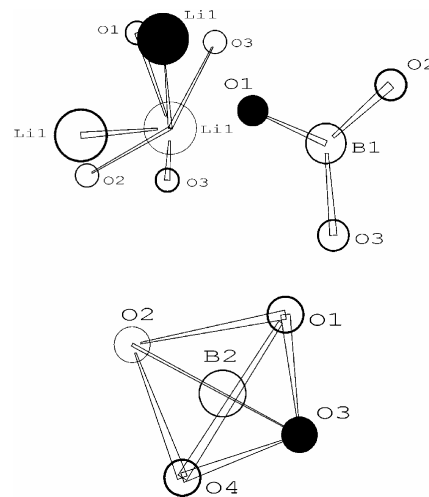


Fig. 5. A model suggested for the local environment of impurity Eu^{3+} centres in the $\text{Li}_2\text{B}_4\text{O}_7$ glass network. For Li1 sites occupied by Eu^{3+} ions, only four oxygen atoms (O1–O4) of the first coordination sphere limited by $r \leq 0.214$ nm are shown.

at the heterovalent substitutions $RE^{3+} \rightarrow Li^+$ and $RE^{3+} \rightarrow Li^+ (Ca^{2+})$ in $Li_2B_4O_7$, CaB_4O_7 and $LiCaBO_3$ can be due to cationic vacancies, which are peculiar for the glass network.

Hence, the local environment of RE^{3+} , in particular, Eu^{3+} centres in the $Li_2B_4O_7$ glass and the same crystal consists of O^{2-} anions with statistically distributed structural parameters (the interatomic distances $Eu^{3+}-O^{2-}$ and the coordination numbers to oxygen) in the first coordination shell leading to so-called ‘positional disorder’. This manifests itself in inhomogeneous broadening of the spectral lines. Additionally, the glass network is characterized by a permanent disturbance of the short-range order, which destroys any middle- and long-range orders. This glassy-like disordering of the second (cationic) coordination sphere around the luminescence centres leads to additional inhomogeneous broadening of the spectral lines. As a result, the optical spectra of the Eu^{3+} centres in the borate glasses are characterized by stronger inhomogeneous broadening, when compared to their crystalline analogues.

Table 1. Experimental lifetimes τ and average interatomic distances d_{RE-O} [32] in the first (oxygen) coordination shell of Eu^{3+} ions at Li(Ca) sites in the $Li_2B_4O_7$, CaB_4O_7 and $LiCaBO_3$ glasses containing 0.5 and 1.0 mol. % Eu_2O_3 .

Glass composition	Eu_2O_3 content, mol. %	Lifetime value τ , ms	Average interatomic distance d_{RE-O} , nm
$Li_2B_4O_7:Eu$	0.5	2.25 ± 0.02	0.279
	1.0	2.26 ± 0.02	
$CaB_4O_7:Eu$	0.5	2.11 ± 0.02	0.262
	1.0	2.12 ± 0.02	
$LiCaBO_3:Eu$	0.5	2.04 ± 0.02	0.258
	1.0	2.07 ± 0.02	

The local structure of the luminescence centres Eu^{3+} suggested by us for the borate glasses correlates well with the spectroscopic data obtained in this work, in particular, with the luminescence lifetime values, which are very sensitive to the local environments. As seen from Table 1, the luminescence lifetime for the Eu^{3+} centres in the $Li_2B_4O_7$, CaB_4O_7 and $LiCaBO_3$ glasses decreases with decreasing average interatomic distances d_{RE-O} in the glass structure. This results correlates with the results of luminescence kinetics known for Dy^{3+} and Tb^{3+} centres [35]. Namely, the latter centres also show a decrease in the lifetimes with decreasing distances d_{RE-O} in the glasses.

4. Conclusions

The borate glasses $Li_2B_4O_7:Eu$, $CaB_4O_7:Eu$ and $LiCaBO_3:Eu$ of high enough optical quality and chemical purity are investigated by the EPR and optical spectroscopy techniques. Basing on our experimental results and the analysis supported by the structural data for those glasses and their crystalline analogues, one can conclude the following:

- The europium impurity is incorporated in the $Li_2B_4O_7$, CaB_4O_7 and $LiCaBO_3$ glass network exclusively as Eu^{3+} ($4f^6$, 7F_0) ions and forms the luminescence Eu^{3+} centres having characteristic optical absorption and photoluminescence spectra.
- All of the transitions in Eu^{3+} centres observed in the UV and visible optical absorption and luminescence (both the excitation and emission) spectra have been successfully identified.

The optical spectra of Eu^{3+} centres in the $\text{Li}_2\text{B}_4\text{O}_7:\text{Eu}$, $\text{CaB}_4\text{O}_7:\text{Eu}$ and $\text{LiCaBO}_3:\text{Eu}$ glasses prove to be almost identical and quite similar to the optical spectra of Eu^{3+} observed in the other borate glasses.

- The optical spectra of Eu^{3+} centres in the $\text{Li}_2\text{B}_4\text{O}_7:\text{Eu}$, $\text{CaB}_4\text{O}_7:\text{Eu}$ and $\text{LiCaBO}_3:\text{Eu}$ glasses are characterized by essential inhomogeneous broadening of the spectral lines. It is caused by statistical distribution of the structural parameters (the interatomic distances $\text{Eu}^{3+}-\text{O}^{2-}$ and the coordination numbers to oxygen) and disturbance of the short-range order (or glassy-like disordering).
- The luminescence decay curves for the Eu^{3+} centres (the ${}^5\text{D}_0 \rightarrow {}^7\text{F}_2$ transition, $\lambda_{\text{max}} \cong 611 \text{ nm}$) in our glasses are satisfactorily described by a single-exponent model. The corresponding lifetimes are 2.25 and 2.26 ms ($\text{Li}_2\text{B}_4\text{O}_7:\text{Eu}$), 2.11 and 2.12 ms ($\text{CaB}_4\text{O}_7:\text{Eu}$), and 2.04 and 2.07 ms ($\text{LiCaBO}_3:\text{Eu}$) for the samples containing 0.5 and 1.0 mol. % Eu_2O_3 , respectively. These results correlate with the relevant data known for the luminescence centres Eu^{3+} in the borate glasses with different compositions.
- The Eu^{3+} luminescence centres are localized at the Li^+ (Ca^{2+}) sites coordinated by positionally disordered O^{2-} anions in the borate glass network. The charge compensation at the heterovalent substitutions $\text{Eu}^{3+} \rightarrow \text{Li}^+$ (Ca^{2+}) can be attributed to the cationic vacancies, $(\text{V}_{\text{Li}})^-$, $(\text{V}_{\text{Ca}})^{2-}$ and $(\text{V}_{\text{B}})^{3-}$, which are available in the borate glass network.
- The multi-site character of the luminescence Eu^{3+} centres in the $\text{Li}_2\text{B}_4\text{O}_7$, CaB_4O_7 and LiCaBO_3 glasses is linked to the Li^+ and Ca^{2+} sites in their structure with different coordination numbers ($N = 4-7$) and statistically distributed $\text{Eu}^{3+}-\text{O}^{2-}$ distances leading to positional disorder.
- Basing on the results obtained, we suggest that the $\text{Li}_2\text{B}_4\text{O}_7$, CaB_4O_7 and LiCaBO_3 glasses activated with Eu^{3+} are promising luminescent materials for the red spectral region.

Acknowledgements

The authors would like to thank Dr. Sci. Adamiv V. T., Dr. Sci. Burak Ya. V. and M. Sc. Teslyuk I. M. from the Institute of Physical Optics (Lviv, Ukraine) for the synthesis of borate glasses and preparation of samples. This work was partly supported by the University of Zielona Góra (Poland).

References

1. Sasaki T, Mori Y, Yoshimura M, Yap Y K and Kamimura T, 2000. Recent development of nonlinear optical borate crystals: key materials for generation of visible and UV light. *Mat. Sci. Eng. R.* **30**: 1–54.
2. Mori Y, Yap Y K, Kamimura T, Yoshimura M and Sasaki T, 2002. Recent development of nonlinear optical borate crystals for UV generation. *Opt. Mater.* **19**: 1–5.
3. Padlyak B V, Adamiv V T, Burak Ya V and Kolcun M, 2013. Optical harmonic transformation in borate glasses with $\text{Li}_2\text{B}_4\text{O}_7$, LiKB_4O_7 , CaB_4O_7 , and LiCaBO_3 compositions. *Physica B.* **412**: 79–82.
4. Padlyak B V, Ryba-Romanowski W, Lisiecki R, Adamiv V T, Burak Ya V and Teslyuk I M, 2012. Synthesis, EPR and optical spectroscopy of the Cr-doped tetraborate glasses. *Opt. Mater.* **34**: 2112–2119.
5. Padlyak B V, Ryba-Romanowski W, Lisiecki R, Adamiv V T, Burak Ya V and Teslyuk I M,

-
- Optical Spectroscopy of Nd-doped Borate Glasses. Proc. Internat. Conf. on Oxide Materials for Electron. Eng. (OMEE-2012), Nat. Univ. "Lviv Polytechnics" (2012). pp. 200–201.
6. Mikulski J, Koepke Cz, Wisniewski K, Padlyak B V, Adamiv V T and Burak Ya V, 2014. Excited state characteristics of the $\text{Li}_2\text{B}_4\text{O}_7$ and KLiB_4O_7 glasses activated by Cr^{3+} ions, *Opt. Mater.* Submitted.
 7. Santiago M, Lavat A, Caselli E, Lester M, Perisinotti L J, de Figuereido A K, Spano F and Ortega F, 1998. Thermoluminescence of strontium tetraborate. *Phys. Status Solidi A.* **167**: 233–236.
 8. Dubovik M F, Korshikova T I, Oseledchik Yu S, Parkhomenko S V, Prosvirnin A L, Svitanko N V, Tolmachev A V and Yavetsky R P, 2005. Thermostimulated luminescence of SrB_4O_7 single crystals and glasses. *Functional Mater.* **12**: 685–688.
 9. Furetta C, Prokic M, Salamon R, Prokic V and Kitis G, 2001. Dosimetric characteristics of tissue equivalent thermoluminescent solid TL detectors based on lithium borate. *Nucl. Instrum. Meth. A.* **456**: 411–417.
 10. Prokic M, 2002. Dosimetric characteristics of $\text{Li}_2\text{B}_4\text{O}_7:\text{Cu,Ag,P}$ solid TL detectors. *Radiat. Prot. Dosimetry.* **100**: 265–268.
 11. Can N, Karali T, Townsend P D and Yildiz F, 2006. TL and EPR studies of Cu, Ag and P doped $\text{Li}_2\text{B}_4\text{O}_7$ phosphor. *J. Phys. D: Appl. Phys.* **39**: 2038–2043.
 12. Senguttuvan N, Ishii M, Shimoyama M, Kobayashi M, Tsutsui N, Nikl M, Dusek M, Shimizu H M, Oku T, Adashi T, Sakai K and Suzuki J, 2002. Crystal growth and luminescence properties of $\text{Li}_2\text{B}_4\text{O}_7$ single crystals doped with Ce, In, Ni, Cu and Ti ions. *Nucl. Instrum. Meth. A.* **486**: 264–267.
 13. Ishii M, Kuwano Y, Asaba S, Asai T, Kawamura M, Senguttuvan N, Hayashi T, Koboyashi M, Nikl M, Hosoya S, Sakai K, Adachi T, Oku T and Shimizu H M, 2004. Luminescence of doped lithium tetraborate single crystals and glass. *Radiat. Meas.* **38**: 571–574.
 14. Zadneprowski B I, Eremin N V and Paskhalov A A, 2005. New inorganic scintillators on the basis of LBO glass for neutron registration. *Functional Mater.* **12**: 261–268.
 15. Burak Ya V, Padlyak B V and Shevel V M, 2002. Radiation-induced centers in the $\text{Li}_2\text{B}_4\text{O}_7$ single crystals. *Nucl. Instrum. Meth. B.* **191**: 633–637.
 16. Burak Ya V, Padlyak B V and Shevel V M, 2002. Neutron-induced defects in the lithium tetraborate single crystals. *Radiat. Eff. Defect Sol.* **157**: 1101–1109.
 17. Burak Ya V, Kopko B N, Lysejko I T, Matkovskii A O, Slipetskii R R and Ulmanis U A, 1989. The center of the colour in $\text{Li}_2\text{B}_4\text{O}_7$ single crystals. *Inorg. Mater.* **25**: 1226–1228.
 18. Blasse G and Grabmaier B C, *Luminescent materials*. Berlin: Springer Verlag, 1994.
 19. Yen W M, Shionoya Sh and Yamamoto H (eds.), *Phosphor handbook*, second ed., Boca Raton: CRC Press, 2006.
 20. Elfayoumi M A K, Farouk M, Brik M G and Elok M M, 2010. Spectroscopic studies of Sm^{3+} and Eu^{3+} co-doped lithium borate glass. *J. Alloy. Compd.* **492**: 712–716.
 21. Kaczmarek S M, 2002. $\text{Li}_2\text{B}_4\text{O}_7$ glasses doped with Cr, Co, Eu and Dy. *Opt. Mater.* **19**: 189–194.
 22. Dubovik M F, Tolmachev A V, Grinyov B V, Grin' L A, Dolzhenkova E F and Dobrotvorskaya M V, 2000. Luminescence and radiation-induced defects in $\text{Li}_2\text{B}_4\text{O}_7:\text{Eu}$ single crystals. *Semiconductor Phys., Quant. Electron. and Optoelectron.* **3**: 420–422.
 23. Lin H, Qin W, Zhang J and Wu C, 2007. A study of the luminescence properties of Eu^{3+} -doped borate crystal and glass. *Solid State Commun.* **141**: 436–439.

-
24. Padlyak B, Grinberg M, Kuklinski B, Oseledchik Y, Smyrnov O, Kudryavtsev D and Prosvirina A, 2010. Synthesis and optical spectroscopy of the Eu- and Pr-doped glasses with $\text{SrO} - 2\text{B}_2\text{O}_3$ composition. *Opt. Appl.* **XL**: 414–426.
 25. Li P, Wang Zh, Yang Z, Guo Q and Li X, 2010. Luminescent characteristics of $\text{LiCaBO}_3:\text{M}$ ($\text{M}=\text{Eu}^{3+}, \text{Sm}^{3+}, \text{Tb}^{3+}, \text{Ce}^{3+}, \text{Dy}^{3+}$) phosphor for white LED. *J. Lumin.* **130**: 222–225.
 26. Gao Y, Shi Ch and Wu Y, 1996. Luminescence properties of $\text{SrB}_4\text{O}_7:\text{Eu}, \text{Tb}$ phosphors. *Mater. Res. Bull.* **31**: 439–444.
 27. Ivankov A, Seekamp J and Bauhofer W, 2006. Optical properties of Eu^{3+} -doped zinc borate glasses. *J. Lumin.* **121**: 123–131.
 28. Su Q, Liang H, Hu T, Tao Y and Liu T, 2002. Preparation of divalent rare earth ions in air by aliovalent substitution and spectroscopic properties of Ln^{2+} . *J. Alloy. Compd.* **344**: 132–136.
 29. Jiao Z, Li S, Yan Q, Wang X and Shen D, 2011. Growth and optical properties of $\text{Eu}^{2+}/\text{Li}^+$ -co-doped SrB_4O_7 single crystals. *J. Phys. Chem. Solids.* **72**: 252–255.
 30. Malchukova E and Boizot B, 2010. Reduction of Eu^{3+} to Eu^{2+} in aluminoborosilicate glasses under ionizing radiation. *Mater. Res. Bull.* **45**: 1299–1303.
 31. Ignatovych M, Holovey V, Watterich A, Vidóczyd T, Baranyaid P, Kelemene A and Chuikoa O, 2004. Luminescence characteristics of Cu- and Eu-doped $\text{Li}_2\text{B}_4\text{O}_7$. *Radiat. Meas.* **38**: 567–570.
 32. Padlyak B V, Mudry S I, Kulyk Y O, Drzewiecki A, Adamiv V T, Burak Y V and Teslyuk I M, 2012. Synthesis and X-ray structural investigation of undoped borate glasses. *Mater. Sci. Poland.* **30**: 264–273.
 33. Podgórska D, Kaczmarek S M, Drozdowski W, Berkowski M and Worsztynowicz A, 2005. Growth and optical properties of $\text{Li}_2\text{B}_4\text{O}_7$ single crystals pure and doped with Yb, Co, and Mn ions for nonlinear applications. *Acta Phys. Pol. A.* **107**: 507–518.
 34. Padlyak B V, Ryba-Romanowski W, Lisiecki R, Pieprzyk B, Burak Ya V, Adamiv V T and Teslyuk I M, Synthesis and spectroscopy of the lithium tetraborate glasses, doped with europium. *Book of Abstracts of The Third International Workshop on Advanced Spectroscopy and Optical Materials (IWASOM'2011)*. 17–22 July 2011, Gdańsk (Poland), 2011.
 35. Padlyak B and Drzewiecki A, 2013. Spectroscopy of the CaB_4O_7 and LiCaBO_3 glasses, doped with terbium and dysprosium. *J. Non-Cryst. Solids.* **367**: 58–69.
 36. Griscom D L, 1980. Electron spin resonance in glasses. *J. Non-Cryst. Solids.* **40**: 211–272.
 37. Brodbeck C M and Bukrey R R, 1981. Model calculations for the coordination of Fe^{3+} and Mn^{2+} ions in oxide glasses. *Phys. Rev. B.* **24**: 2334–2342.
 38. Hoefdraad H E, 1975. The charge-transfer absorption band of Eu^{3+} in oxides. *J. Solid State Chem.* **15**: 175–177.
 39. Carnall W T, Fields P R and Rajnak K, 1968. Electronic energy levels of the trivalent lanthanide aquo ions. IV. Eu^{3+} . *J. Chem. Phys.* **49**: 4450–4455.
 40. Carnall W T, Beitz J V, Crosswhite H, Rajnak K and Mann J B, Spectroscopic properties of the f-elements in compounds and solution in: S.P. Sinha (ed.). *Systematic and the properties of the lanthanides*. Reidel Dordrecht, 1983. pp. 389–450.
 41. Ronda C R, Luminescence: from theory to applications. Weinheim: Wiley, 2008.
 42. Binnemans K and Görrler-Walrand C, 1996. Application of the Eu^{3+} ion for site symmetry determination. *J. Rare Earth.* **14**: 173–180.
 43. Babu P and Jayasankar C K, 2000. Optical spectroscopy of Eu^{3+} ions in lithium borate and lithium fluoroborate glasses. *Physica B.* **279**: 262–281.

-
44. Lavín V, Rodríguez-Mendoza UR, Martín IR and Rodríguez VD, 2003. Optical spectroscopy analysis of the Eu^{3+} ions local structure in calcium diborate glasses. *J. Non-Cryst. Solids*. **319**: 200–216.
 45. Lin H, Yang D, Liu G, Ma T, Zhai B, An Q, Yu J, Wang X, Liu X and Yue-Bun Pun E, 2005. Optical absorption and photoluminescence in Sm^{3+} - and Eu^{3+} -doped rare-earth borate glasses. *J. Lumin.* **113**: 121–128.
 46. Venkatramu V, Babu P and Jayasankar C K, 2006. Fluorescence properties of Eu^{3+} ions doped borate and fluoroborate glasses containing lithium, zinc and lead. *Spectrochim. Acta A*. **63**: 276–281.
 47. Jayasankar C K, Ramanjaneya Setty K, Babu P, Tröster Th, Holzapfel W B, 2004. High-pressure luminescence study of Eu^{3+} in lithium borate glass. *Phys. Rev. B*. **69**: 214108–7.
 48. Thulasiramudu A, Buddhu S, 2007. Optical characterization of Eu^{3+} and Tb^{3+} ions doped zinc lead borate glasses. *Spectrochim. Acta A*. **66**: 323–328.
 49. Witkowska A, Padyak B and Rybicki J, 2008. An EXAFS study of the local structure of rare-earth luminescence centres in the $3\text{CaO}-\text{Ga}_2\text{O}_3-3\text{GeO}_2$ glass. *Opt. Mater.* **30**: 699–702.
 50. Padyak B V, Sergeev N A, Olszewski M, Adamiv V T and Burak Ya V, 2014. ^{11}B and ^7Li MAS NMR spectroscopy of glassy and crystalline borate compounds. *Phys. Chem. Glasses: Eur. J. Glass Sci. Technol. B*. **55**: 25–33.
 51. Krogh-Moe J, 1968. Refinement of the crystal structure of lithium diborate, $\text{Li}_2\text{O} \cdot 2\text{B}_2\text{O}_3$. *Acta Crystallogr. B*. **24**: 179–181.
 52. Krogh-Moe J, 1964. The crystal structure of strontium diborate, $\text{SrO} \cdot 2\text{B}_2\text{O}_3$. *Acta Chem. Scand.* **18**: 2055–2060.
 53. Wu L, Chen X L, Li H, He M, Dai L, Li X Z and Xu Y P, 2004. Structure determination of a new compound LiCaBO_3 . *J. Solid State Chem.* **177**: 1111–1116.

Padyak B.V., Kindrat I.I., Protsiuk V.O. and Drzewiecki A. 2014. Optical spectroscopy of $\text{Li}_2\text{B}_4\text{O}_7$, CaB_4O_7 and LiCaBO_3 borate glasses doped with europium. *Ukr.J.Phys.Opt.* **15**: 103–117.

Анотація. Досліджено і проаналізовано оптичні властивості (оптичне поглинання, спектри випромінювання та збудження, а також кінетику люмінесценції) серії зразків боратних стекол $\text{Li}_2\text{B}_4\text{O}_7$, CaB_4O_7 і LiCaBO_3 , легованих Eu . Досліджувані стекла високої хімічної чистоти та оптичної якості зі складами $\text{Li}_2\text{B}_4\text{O}_7:\text{Eu}$, $\text{CaB}_4\text{O}_7:\text{Eu}$ і $\text{LiCaBO}_3:\text{Eu}$ було отримано з відповідних полікристалічних сполук в атмосфері повітря з використанням стандартної технології скловаріння. Домішку Eu додавали до боратних сполук у вигляді Eu_2O_3 в кількостях 0,5 і 1,0 мол. %. На основі даних ЕПР і аналізу оптичних спектрів показано, що домішка європію входить у структуру скла зі складами $\text{Li}_2\text{B}_4\text{O}_7$, CaB_4O_7 і LiCaBO_3 виключно у вигляді йонів Eu^{3+} ($4f^6$, 7F_0). Усі переходи $4f-4f$, спостережені для центрів Eu^{3+} , ідентифіковано в спектрах оптичного поглинання та люмінесценції досліджуваних зразків скла. Найінтенсивніша смуга випромінювання йонів Eu^{3+} із максимумом 611 нм (перехід $^7F_2 \rightarrow ^5D_0$) характеризується одноекспоненційною кінетикою загасання з типовими часами життя, які залежать від складу скла і локальної структури центрів люмінесценції Eu^{3+} . Особливості електронної та локальної структури домішкових центрів Eu у склах $\text{Li}_2\text{B}_4\text{O}_7$, CaB_4O_7 і LiCaBO_3 обговорено в плані порівняння з даними інших робіт для легованих Eu боратних монокристалів, полікристалічних сполук з аналогічними хімічними складами та боратних стекол інших складів.